



Joint Demosaicking / Rectification of Fisheye Camera Images using Multi-color Graph Laplacian Regularization

Fengbo Lan^{*}, Cheng Yang^{*}, Gene Cheung^{*}, Jack Z. G. Tan[†]

^{*}Dept of EECS, York University, Toronto, Canada

[†]Kandao Technology, Sydney, Australia

Session: 3D-03: Image and Video Processing Augmented and Virtual Reality

October 26, 2020



Overview

- 1 Motivation and Contribution
- 2 Related Works
- 3 Problem Formulation and Algorithm
- 4 Experiment
- 5 Conclusion

Motivation

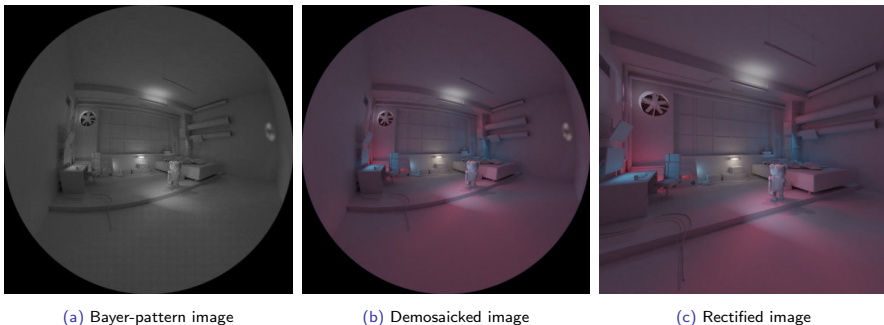


Figure 1: Conventional processing pipeline

- Conventional processing pipeline for fisheye camera images:
 - ▶ (a) to (b): Demosaicking on Bayer-patterned grid
 - ▶ (b) to (c): Mapping demosaicked pixels to a rectified image grid
- Interpolate *twice* lead to errors accumulation and correlated noise

Contribution

We propose:

- Joint demosaicking / rectification method
 - ▶ Image interpolation is performed *once*
 - ▶ Noise pollution is limited
- A synthesized dataset for fisheye camera demosaicking and rectification
 - ▶ Images rendered with 2 camera models
 - ▶ 140 paired images generated with 4 3-D models
 - ▶ The inverse mapping matrix for rectification

Related Works

- Joint demosaicking / denoising methods¹²³
- Graph spectral image methods
 - ▶ Work well in many image applications, e.g., denoising⁴, deblurring⁵, JPEG de-quantization⁶
 - ▶ Motivate us to develop **accurately estimated gradient** method

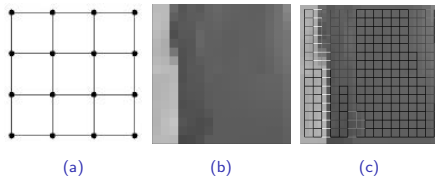


Figure 2: (a) Square grid graph; (b) a 16×16 image block, and (c) an example of graph superimposed onto it.

¹K. Hirakawa and T. W. Parks, "Joint demosaicing and denoising," IEEE Transactions on Image Processing, vol. 15, no. 8, pp. 2146–2157, Aug 2006.

²L. Zhang, X. Wu, and D. Zhang, "Color reproduction from noisy cfa data of single sensor digital cameras," IEEE Transactions on Image Processing, vol. 16, no. 9, pp. 2184–2197, Sep. 2007.

³M. Gharbi, G. Chaurasia, S. Paris, and F. Durand, "Deep joint demosaicing and denoising," ACM Transactions on Graphics, vol. 35, no. 6, pp. 191:1–191:12, Nov. 2016.

⁴J. Pang and G. Cheung, "Graph Laplacian regularization for image denoising: Analysis in the continuous domain," IEEE Transactions on Image Processing, vol. 26, no. 4, pp. 1770–1785, April 2017.

⁵Y. Bai, G. Cheung, X. Liu, and W. Gao, "Graph-based blind image deblurring from a single photograph," IEEE Transactions on Image Processing, vol. 28, no. 3, pp. 1404–1418, March 2019.

⁶X. Liu, G. Cheung, X. Ji, D. Zhao, and W. Gao, "Graphbased joint dequantization and contrast enhancement of poorly lit JPEG images," IEEE Transactions on Image Processing, vol. 28, no. 3, pp. 1205–1219, March 2019.

Problem Formulation

Maximum a Posteriori (MAP) Formulations for Image Restoration

Definition

- $\mathbf{y} \in \mathbb{R}^M$: input M -pixel Bayer-pattern patch
- $\mathbf{H} \in \mathbb{R}^{N \times M}$: weight matrix used for interpolation
- $\mathbf{x} \in \mathbb{R}^N$: target square pixel patch in the rectified grid
- $\mathbf{L}_x \in \mathbb{R}^{N \times N}$: graph Laplacian matrix

- Problem formulated with GLR⁷:

$$\min_{\mathbf{x}} \|\mathbf{H}\mathbf{y} - \mathbf{x}\|_2^2 + \mu \mathbf{x}^\top \mathbf{L}_x \mathbf{x} \quad (1)$$

- Fix \mathbf{H} and \mathbf{L}_x , it is solved with close form solution:

$$(\mathbf{I} + \mu \mathbf{L}_x) \mathbf{x} = \mathbf{H}\mathbf{y} \quad (2)$$

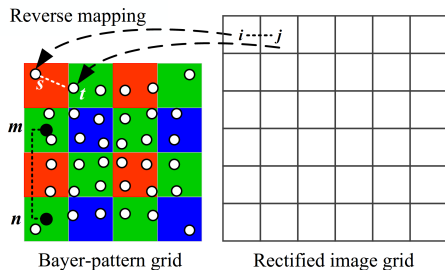


Figure 3: Reverse mapping from the rectified grid to the Bayer-patterned grid.

⁷J. Pang and G. Cheung, "Graph Laplacian regularization for image denoising: Analysis in the continuous domain," IEEE Transactions on Image Processing, vol. 26, no. 4, pp. 1770–1785, April 2017.

Algorithm

Graph Construction

Definition

- $v_{i,j}^k$: associate weight computed with handcrafted features
- $\delta_{i,j}^k$: gradient (difference) of the pixel values on the Bayer-pattern grid
- Defined weight $w_{i,j}$ as:

$$w_{i,j} = \exp \left\{ -\frac{\Delta_{i,j}^2}{\sigma_w^2} \right\} \quad (3)$$

- Estimate gradient $\Delta_{i,j} \in \mathbb{R}$ via *maximum likelihood estimation* (MLE):

$$\Delta_{i,j}^* = \frac{1}{V} \sum_{k=1}^K v_{i,j}^k \delta_{i,j}^k \quad (4)$$

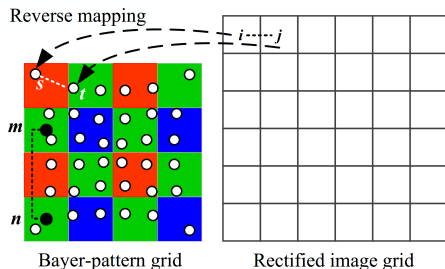
Algorithm

Noise Model for Inter-pixel Gradient

Definition

- (i, j) : paired pixels in the rectified grid.
 - (s, t) : correspond pixels of pair (i, j) in Bayer-pattern image
 - $\mathcal{N}_{i,j}$: spatial neighborhood surrounding (s, t)
 - $(m, n) \in \mathcal{N}_{i,j}$: pair of adjacent pixels of the same color
-
- Compute gradient for pair $(m, n) \in \mathcal{N}_{i,j}$ as:

$$\delta_{i,j}^{m,n} = y_m - y_n \quad (5)$$



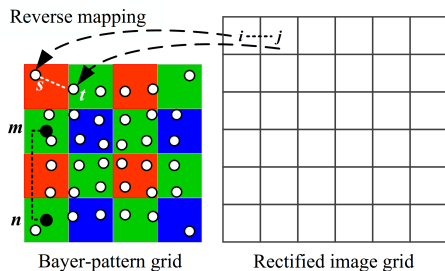
Algorithm

Noise Model for Inter-pixel Gradient

Features considered for associated weight:

- Euclidean distance between (m, n) and (s, t)
- Relative angle between (m, n) and (s, t)
- Color correlation

$$v_{i,j}^{m,n} = \exp \left\{ -\frac{\|I_s - I_m\|_2^2 \|I_t - I_n\|_2^2}{\sigma_v^2} \right\} \cos \theta_{s,t}^{m,n} \rho_{s,t}^{m,n} \quad (6)$$



Experiment

Experimental Setup

- Test on Multi-FoV image dataset⁸ and in-house dataset⁹:
 - ▶ 5 images from scene room and 25 images from scene city⁸
 - ▶ 3 images from each scene (box, chair, skull and teddy)
 - ▶ Removed pixels to generate Bayer-patterned images
 - ▶ Add Gaussian noise (variance $\sigma = 15$)
- Competing schemes:
 - ▶ For demosaicking: (1) bilinear interpolation (2) a high quality linear (HQL) filter¹⁰
 - ▶ For rectification: bilinear interpolation method

⁸Z. Zhang, H. Rebecq, C. Forster, and D. Scaramuzza, "Benefit of large field-of-view cameras for visual odometry," in 2016 IEEE International Conference on Robotics and Automation (ICRA), May 2016, pp. 801–808.

⁹The dataset is available at: <https://github.com/fengbolan/York-Fisheye-Image-Rectification-Dataset>

¹⁰H. S. Malvar, L. He, and R. Cutler, "High-quality linear interpolation for demosaicing of bayer-patterned color images," in 2004 IEEE International Conference on Acoustics, Speech, and Signal Processing, May 2004, vol. 3, pp. iii–485.

Experiment

Experimental Results

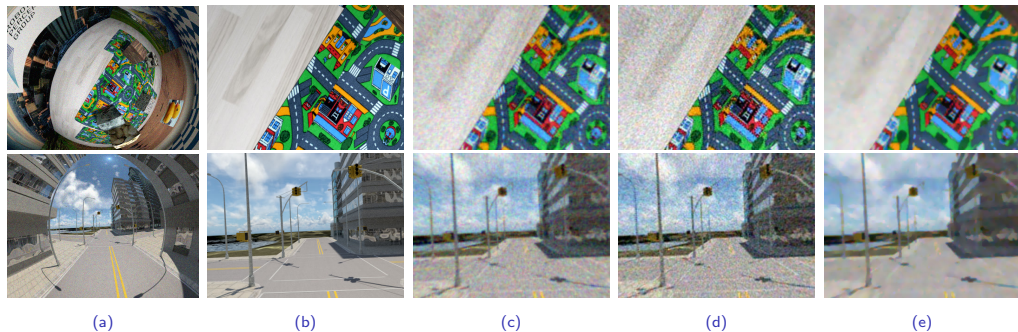


Figure 4: Results of demosaicking and rectification for room and city. (a) Ground truth fisheye camera image. (b) Ground truth pinhole image. (c) Demosaicking and rectification using the bilinear method. (d) Demosaicking using high quality linear interpolation (HQL) and rectification using the bilinear method. (e) Our proposed joint demosaicking / rectification method.

Experiment

Experimental Results

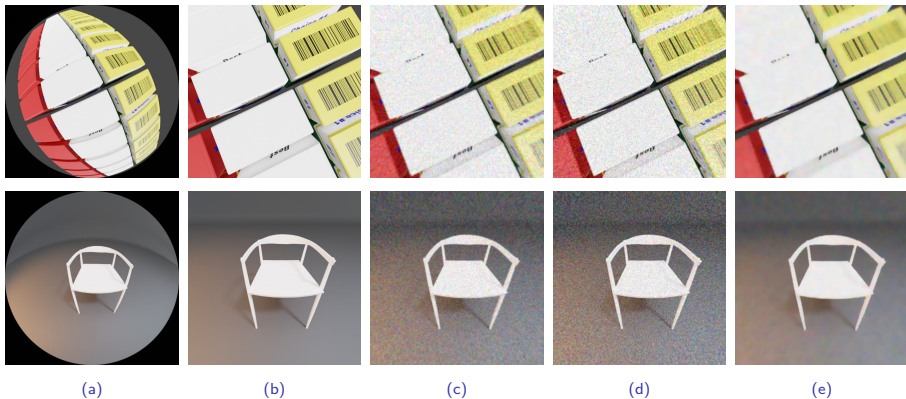


Figure 5: Demosaicking and rectification result of the in-house dataset, where the images are generated from the 3-D models: box and chair. (a) Ground truth fisheye camera image. (b) Ground truth pinhole image. (c) Demosaicking and rectification using the bilinear method. (d) Demosaicking using HQL interpolation and rectification using the bilinear method. (e) Our proposed joint demosaicking / rectification method.

Experiment

Experimental Results

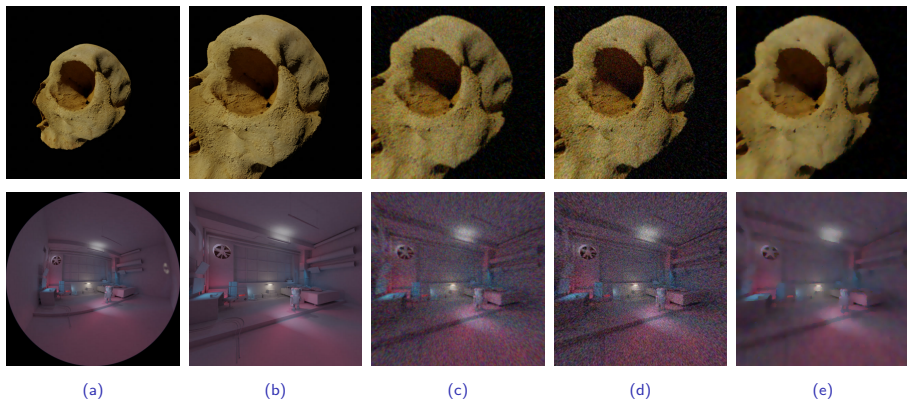


Figure 6: Demosaicking and rectification result of the in-house dataset, where the images are generated from the 3-D models: `skull` and `teddy`. (a) Ground truth fisheye camera image. (b) Ground truth pinhole image. (c) Demosaicking and rectification using the bilinear method. (d) Demosaicking using HQL interpolation and rectification using the bilinear method. (e) Our proposed joint demosaicking / rectification method.

Experiment

Experimental Results

Table 1: Average SSIM¹¹ and PSNR of images from 6 scenes under noise level $\sigma = 15$. 5 and 25 images from room and city respectively from the Multi-FoV image dataset¹² were used. 3 images each from scene box, chair, skull and teddy from our in-house dataset were used. For demosaicking, bilinear interpolation and high quality linear (HQL) method¹³ were used for comparison. In both cases, bilinear was used for rectification.

Scene name	SSIM ¹¹			PSNR (dB)		
	Bilinear	HQL ¹³	Proposed	Bilinear	HQL ¹³	Proposed
room ¹²	0.710	0.702	0.788	20.76	21.04	20.91
city ¹²	0.550	0.557	0.622	24.24	24.25	24.77
box	0.599	0.531	0.849	21.88	21.20	22.52
chair	0.601	0.505	0.916	26.68	25.35	29.80
skull	0.648	0.556	0.861	26.02	24.92	27.58
teddy	0.722	0.641	0.919	27.63	26.10	31.63

¹¹Z. Wang, A. Bovik, H. Sheikh, and E. Simoncelli, "Image quality assessment: From error visibility to structural similarity," in IEEE Transactions on Image Processing, August 2005, vol. 13, no.4, pp. 600–612.

¹²Z. Zhang, H. Rebecq, C. Forster, and D. Scaramuzza, "Benefit of large field-of-view cameras for visual odometry," in 2016 IEEE International Conference on Robotics and Automation (ICRA), May 2016, pp. 801–808.

¹³H. S. Malvar, L. He, and R. Cutler, "High-quality linear interpolation for demosaicing of bayer-patterned color images," in 2004 IEEE International Conference on Acoustics, Speech, and Signal Processing, May 2004, vol. 3, pp. iii–485.

Conclusion

- We propose:
 - ▶ Joint demosaicking and rectification method based on accurate gradient estimation
 - ▶ Synthesized dataset for fisheye camera demosaicking and rectification
- Future work: A journal version is in preparation
 - ▶ Larger dataset of simulating lens distortion
 - ▶ Real sensor noise simulation (signal-dependent noise)
 - ▶ Learning-based method for learning parameters

The dataset is available at: :

<https://github.com/fengbolan/York-Fisheye-Image-Rectification-Dataset>

If you have any questions, please contact:

Gene Cheung: genec@yorku.ca

Fengbo Lan: fengbo@yorku.ca